IOPscience iopscience.iop.org

Home Search Collections Journals About Contact us My IOPscience

Ballistic transport in a one-dimensional system with an arbitrary longitudinal potential

This article has been downloaded from IOPscience. Please scroll down to see the full text article.

1989 J. Phys.: Condens. Matter 1 5421

(http://iopscience.iop.org/0953-8984/1/32/011)

View the table of contents for this issue, or go to the journal homepage for more

Download details:
IP Address: 171.66.16.93
The article was downloaded on 10/05/2010 at 18:36

Please note that terms and conditions apply.

J. Phys.: Condens. Matter 1 (1989) 5421–5427. Printed in the UK

Ballistic transport in a one-dimensional system with an arbitrary longitudinal potential

L Martin-Moreno† and C G Smith‡
† Department de Fisica de la Materia Condensa (C-12), Universidad Autónoma de Madrid, 28049 Madrid, Spain
‡ Cavendish Laboratory, University of Cambridge, Cambridge CB3 0HE, UK

Received 10 March 1989, in final form 9 May 1989

Abstract. We present a theoretical study of the transport through a narrow constriction in a two-dimensional gas of independent electrons, when a potential of arbitrary shape in the longitudinal direction is placed inside the channel. In particular we model a double-barrier potential obtaining a reasonable agreement between our theory and the experiment of Smith and co-workers. The resonant structure observed in the conductance is found to be very sensitive to sample disorder. Predictions are made for a single potential barrier placed within the split gate.

1. Introduction

It has been demonstrated that the 2D electron gas in a GaAs–AlGaAs heterojunction can be manipulated in a controlled way by the ‘electrostatic squeezing’ arising from a potential applied to a split Schottky gate (Thornton *et al* 1986). In this way a transition from 2D to 1D can be induced and, if the length of the 1D channel is less than the scattering length, ballistic transport can be observed with the conductance showing steps of height $2e^2/h$ (van Wees *et al* 1988, Wharam *et al* 1988). Subsequently Smith *et al* (1988) studied the conductance of a similar system in which the metallisation was such that two narrow potential barriers were introduced into a 1D electron gas; see figure 1. Increasing the magnitude of the potential results in the formation of a lateral quantum box of side 0.3 μm, in which the electron gas is quantised in all three directions.

In this paper we calculate electron transport using a simple but realistic model that takes into account the channel geometry, and the potential shape inside the channel, and we compare the results with the experiments of Smith *et al* (1988). We model the experimental geometry by two wide regions of width W in the X–Y plane joined by a narrow channel of length L and width $W' \ll W$. The channel walls are assumed to be infinite potentials and along the channel there is a potential $V(x)$ of arbitrary shape. We shall use the effective-mass approximation, so the electrons are considered free and independent particles. The model is an extension of the WNW (wide–narrow–wide) model used previously by Szafer and Stone (1989) (from where the nomenclature has been taken), and by Kirczenow (1989) which was developed to explain the resistance quantisation. (In those calculations the only cases considered were, $V(x) = 0$ (Szafer

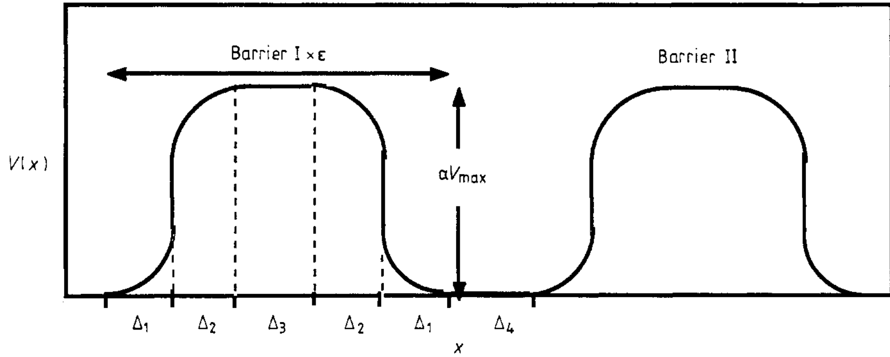

Figure 1. The potential shape inside the barriers used in the calculations. All the lengths in barrier II are multiplied by a factor α while the height is multiplied by a factor ε. α is a measure of the barrier height anisotropy and ε is a measure of the barrier width anisotropy. Both ε and $\alpha = 1$ for figures 2 and 3 (symmetric barriers), but change in 4 and 5. The various lengths that define the potential are: $W = (0.38 + 0.158\ V_g)\ \mu\text{m}$, $\Delta_1 = 25$ nm, $\Delta_3 = (a - 0.158\ V_g)\ \mu\text{m}$ with $a = -0.039$, $\Delta_4 = 0.5\ \mu\text{m} - 2(\Delta_1 + \Delta_2) - \Delta_3$, $V_{max} = (-6.324 - 21.23\ V_g)$ meV and $V_g < -0.6$ V. V_{max} is the maximum of the channel potential, and in all the equations V_g is in volts.

and Stone 1989) and $V(x)$ = constant (Kirczenow 1988).) We mention here that the self-consistent calculations of Laux *et al* (1988) point to a parabolic–flat–parabolic confining potential in the y direction, where only the flat region width changes with gate voltages. Wharam *et al* (1989) used this potential for calculating the gate voltage and magnetic field dependence of the steps of conductivity and obtained excellent agreement with experiment. Such a potential makes the calculations much more complicated and requires a great deal of computer time; however, Kirczenow (1989) using a parabolic confining potential gets qualitatively the same results as in the infinite-square-well confining potential for the case $V(x)$ = constant.

2. The Formalism

We adopt the formalism and methodology of Szafer and Stone (1989), but extend it to cover the case of varying $V(x)$ by regarding the channel as made up of many short segments in series. The potential within each segment is constant (so in fact we are discretising the potential), and the transmission and reflection coefficients are calculated and matched not only at the entrance and exit of our channel, but at each of the internal segment boundaries as well. A transfer matrix formalism enables us to calculate the transmission kernel A_{mn} for the entire channel (Szafer and Stone (1989)). We also adopt a partial decoupling of the equation which they refer to as the mean-field theory (MFT); this leads to an error in the conductance of the order of 5–10%.

As an extension of the Szafer and Stone case, we can write the current, when a small drift potential is applied between the wide regions, as

$$J = \sum_w \int_{E_F}^{E_F+eV} j_{nw}\, \mathrm{d}E \qquad q_w \leqslant q_F \tag{1}$$

with

$$j_{nw} = \frac{eh}{m^*}\left[\left(\frac{k_n^{(i)} + k_n^{(i)*}}{2}\right)(t_{nw}^{(i)} t_{nw}^{(i)*} - r_{nw}^{(i)} r_{nw}^{(i)*}) + \left(\frac{k_n^{(i)} - k_n^{(i)*}}{2}\right)(t_{nw}^{(i)} r_{nw}^{(i)*} - t_{nw}^{(i)*} r_{nw}^{(i)})\right] \tag{2}$$

where the summations are as follows: w denotes the lateral quantisation index within the wide regions and the summation is restricted to those values of wavevector that give an energy less than the Fermi energy; the discrete levels within the channel are indexed by n in the exit segment, and relevant transmission coefficient $t_{nw}^{(i)}$ is taken from the previous calculations, i denoting the fact that the transfer matrices of the i internal segments have been multiplied to give $t_{nw}^{(i)}$. From this we extract the conductance G as

$$G(E_{\mathrm{F}}, T=0) = \lim_{v=0} \frac{J}{V} = \sum_{q_w \leq q_{\mathrm{F}}} e j_{nm}. \tag{3}$$

This method of calculating the conductance is equivalent to using the Landauer type formula $G = (e^2/h)\,\mathrm{Tr}(\mathbf{tt}^*)$ derived by Fisher and Lee (1981), and Economou and Soukoulis (1981). This seems to be the physically relevant version, at least before a better understanding of how to introduce the physics of reservoirs in the calculations appears. The Buttiker *et al* (1985) formula gives the same result for the case where $W \gg W'$.

The temperature dependence of the conductance is approximated by

$$G(E_{\mathrm{F}}, T) = \int_0^{\infty} G(E, T=0)(-\delta f(E_{\mathrm{F}}, E)/\delta E)\,\mathrm{d}E \tag{4}$$

where

$$f(E_{\mathrm{F}}, E) = \{1 + \exp[(E - E_{\mathrm{F}})/kT]\}^{-1}. \tag{5}$$

The transmission coefficient in a zero-dimensional device is rich in structure and the resulting resonances in the conductance can have a stronger temperature evolution than those calculated from this equation because, not only does the Fermi distribution change, but also the inelastic scattering time alters, which affects the resonances when the scattering time becomes shorter than the tunnelling time (Payne 1988).

3. The longitudinal channel potential

In order to do a semiquantitative comparison with the experiment of Smith *et al* (1988), we have modelled a realistic longitudinal potential inside the channel. Our chosen potential shape is depicted in figure 1 where the curves are sine-like functions. In this model the regions of width Δ_1 reflect the potential curvature found in the Laux *et al* (1988) calculations, while the regions of width Δ_2 simulate the capacitance edge effects. These edge effects also reduce the potential under the narrow-gate regions, so at gate voltages, which have defined the channel under the large gate areas, the barriers are still lower than the Fermi level. The barrier height is expected to depend on the distance between the gate regions and the 2DEG (70 nm in this case), and on the doping of the GaAs and AlGaAs layers over the 2DEG. It is difficult to estimate its value, and it will be fitted later. The variation of Δ_3 and W with gate voltage has been estimated from the experiment of Wharam *et al* (1988). The dependence of the maximum of the channel potential with gate voltage has been adjusted assuming a linear relationship, obtained by fitting the potentials and voltages for the sixth-channel disappearance and pinch-off,

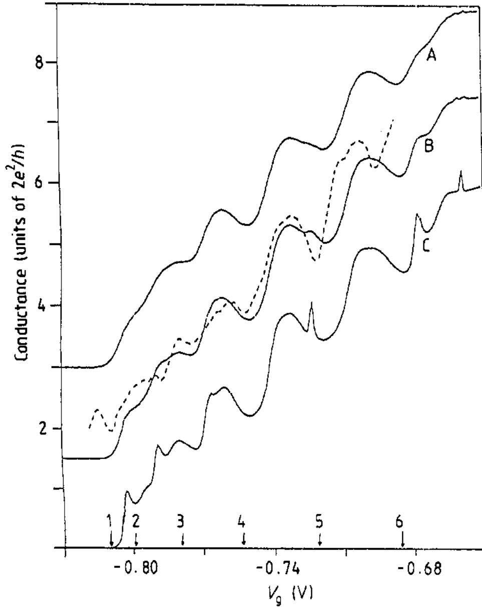

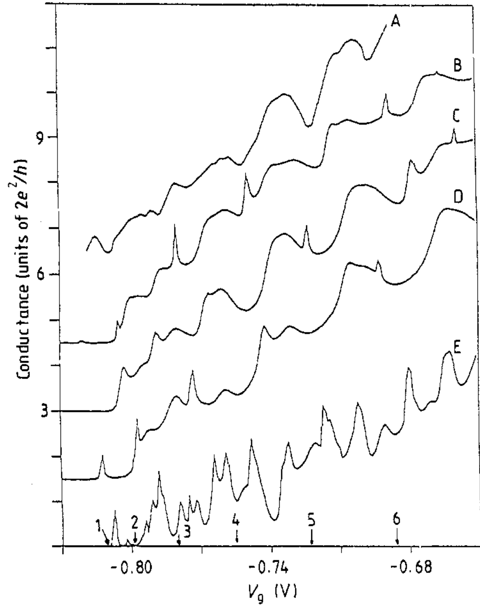

Figure 2. The G–V_g curves for: (curve A) experimental results for $T = 330$ mK; (curve B, C and D) the model of figure 1, with $\Delta_2 = 20, 35, 70$ nm respectively, (curve E) a square potential version of the model of figure 1 (see the text). All model calculations are for $T = 0$ mK. The arrows marked from 1 to 6 indicate the voltage at which classically channels 1 to 6 disappear. Each curve has been shifted with respect to the preceding curve by $3e^2/h$ for clarity.

Figure 3. The temperature dependence of the G–V_g curves. The broken curve is the experimental result for $T = 330$ mK, and the full curves are calculated ones. Curve A is calculated for $T = 500$ mK, curve B for $T = 300$ mK and curve C for $T = 0$ K. The arrows have the same meaning as in figure 2. The curves for different temperatures have been shifted by $3e^2/h$ each time for clarity.

i.e. fixing the voltage values for the sixth and first arrows in figure 2. The rest of the parameters were taken assuming that the lengths have their nominal lithographic values when the channel is defined at $V_g = -0.6$ V. All the appropriate lengths are given in figure 1. $E_F = 11$ meV and $m^* = 0.067$ (in electron mass units) for electrons in the system used in the experiment. The parameters α and ε in figure 1 are used to change the potential shape, and introduce disorder into the system.

4. Results

4.1. Effect of gate voltage

In figure 2 the experimental dependence of conductance versus gate voltage for $T = 330$ mK are shown (curve A). The calculated results for the symmetric barriers, with different values of Δ_2 (the capacitor edge effect), are shown for $T = 0$ (curves B–E). The calculated variation of G with V_g for the bigger value of Δ_2 typically shows a stepped structure with a resonant peak over each step. This is because when $E_F - V_{max}$ is smaller than the minimum energy in the nth band, E_n, the electron in the nth band finds a large classically forbidden region, and does not carry current unless it finds a resonant state.

As the Δ_2 value gets smaller, tunnelling effects are more important, and the G versus V_g curve is less step-like. However, when the smooth region of the potential (with length $\Delta_1 + \Delta_2$) is shorter than the Fermi wavelength (45 nm in this paper), the reflection is greatly enhanced from the now sharp potential corners, resulting in a smaller total conductance which contains many resonances as can be seen from curve E of figure 2. This graph shows the G–V_g dependence with a potential inside the channel composed of two square potentials with width $2\Delta_2 + \Delta_3$, separated by a zero-potential region of width $2\Delta_1 + \Delta_4$ symmetrically placed in a channel of length $4\Delta_1 + 4\Delta_2 + 2\Delta_3 + \Delta_4$, and with the same gate voltage dependence for the two barrier heights as for curves B–D. The structure is very different from that observed exprimentally. Using these curves we have chosen the value $\Delta_2 = 35$ nm (curve C), as the value that best fits the experimental result (curve A), and therefore has been used for the following results. As the gates are separated from the 2DEG by 70 nm a value of 35 nm for the rounding due to capacitance edge effects is not unreasonable.

The structure seen in the conductance, when the gate voltage is swept to negative values, depends critically on the rounding assumed for the top region of the potential barriers, Δ_2. When this rounding becomes smaller than the Fermi wavelength the transmission coefficient for each sub-band has many sharp dips that approach zero and are closely spaced in gate voltage. However, simulations show that the structure seen is not at all critically dependent on the rounding of the bottom of the barrier, Δ_1.

4.2. Effect of temperature

The temperature dependence of the conductance versus gate voltage is shown in figure 3. The resonances are smeared, with the dips in conductance tending to higher values and the maxima to smaller ones. This differs from the experiment in which the dips in conductance quickly disappear as the temperature is raised. The dips in conductance result from a build up of a localised state between the barriers which is destroyed at higher temperatures, when the inelastic length becomes longer than twice the separation of the barriers. In our simulations we have not included the effect of a changing inelastic length, but have just used equations (4) and (5).

4.3. Effect of asymmetry on the double-barrier potential

We simulate asymmetry of the gate lines by changing the parameters α and ε, defined in figure 1. Although in real systems differences in the gate linewidths implies different channel potential widths and different channel potential maxima, we shall show these effects separately for conceptual clarity.

The effect on the G–V_g curve of a barrier height asymmetry (values of α different from 1) is shown in the curves A and B of figure 4. For small deviations of α from 1, i.e. when the maximum of one of the barriers is slightly bigger than the other, the resonance diminishes greatly. For $\alpha = 0.9$, the resonances have disappeared and the conductance is more step-like. This effect explains why only a small number of samples tested show such strong peaks in the G–V_g curve. Only those in which the two narrow-gate lines perpendicular to the current are nearly equal in width will show resonances.

The effect on the G–V_g curve of asymmetry in the width of the barriers ($\varepsilon \neq 1$), is presented in curves D and E of figure 4. The width difference diminishes the resonances and the curve is smeared; however, this effect is much smaller than that resulting from the different barrier heights, discussed before. When the difference in width is 40%

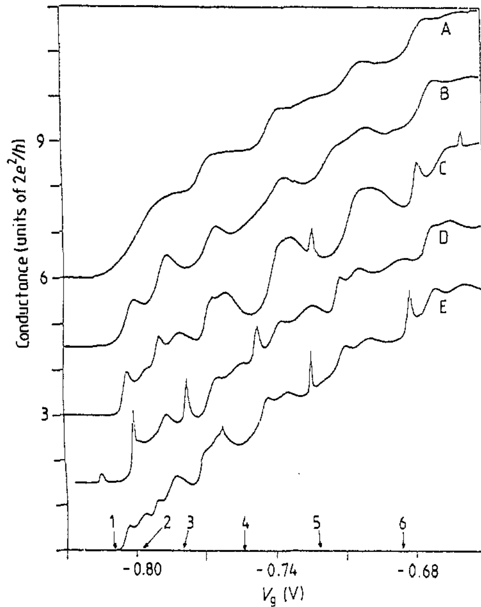

Figure 4. The G–V_g curves showing the variation with asymmetry in the channel potential. For curves A and B, $\alpha = 0.9$, 0.95 respectively, and the barrier widths are equal. For curves D and E, $\varepsilon = 1.2$, 1.4 respectively, and the barrier maxima are equal. Curve C is the result for the symmetric double barrier ($\alpha = 1$, $\varepsilon = 1$). The arrows have the same meaning as in figure 2. Each curve has been shited with respect to the preceding one by $3e^2/h$.

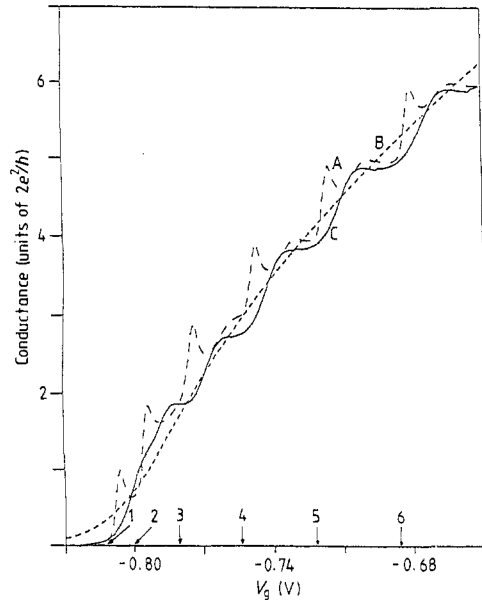

Figure 5. The G–V_g curves for one single barrier inside the channel ($\varepsilon = 0$) for: (A) the gate line-widths used in the experiment; (B) narrower gate lines; (C) wider gates lines (see the text). The arrows have the same meaning as in figure 2.

resonances can still be observed. We point out that the results presented in the curves D–E can change greatly when the model parameters are changed; for example, for narrow-gate lines, the G–V_g curve is smooth, but by making ε bigger step-like structure develops.

4.4. *A single barrier*

The $\alpha = 0$ case (only one barrier inside the channel) is shown in figure 5 for three different widths of the gate lines. In curve B, the width is the same as used in figures 1–4, and the conductance versus gate voltage is step-like, due to the removing of sub-bands when the gate voltage gets smaller. The comparison between this result and the two barriers with $\alpha = 0.9$ shows that the more relevant features of the result are due to the region near the potential top. Curve B in figure 5 is the simulation for a narrower gate line. For this a value of $\Delta_3 = (-0.095 - 0.158\ V_g)\ \mu$m is used and because tunnelling is important a smoother curve results. For curve C $\Delta_3 = (0.04 - 0.158\ V_g)\ \mu$m which is a wider line leading to resonances due to reflections in the ends. This change in the G–V_g curve is similar to the one found by Szafer and Stone (1989), and Kirzcenow (1988) in the $V(x) = 0$ case, when the channel length is decreased. Although in the case presented

here the results are less easily explained (because there are more length scales involved, and the potential inside the channel does not have sharp corners).

Simulations therefore show that with a single fine line the structure in conductance versus gate voltage becomes less dramatic as the linewidth of the barrier is reduced.

5. Conclusion

In summary, we have presented a model for calculating the conductance in a 2DEG of independent electrons with a constriction, when a potential inside, of arbitrary shape in the longitudinal direction, is defined. A double-barrier potential has been modelled and we obtained reasonable agreement with the experiment of Smith *et al* (1988). In order to get this agreement, it is very important to assume a rounded potential top region which extends over half the distance that the gate is separated from the 2DEG. This is due to capacitance edge effects. The experimental results can be explained in terms of a variation in the transmission coefficients induced by the barriers, and were found to be very sensitive to the sample asymmetry. Predictions have been made for a single barrier inside the channel and it was shown that no better quantisation in the conductance, with gate voltage, is expected in this case than in the case in which the sub-bands are removed by changing the channel width. This point deserves further study and experimental confirmation.

Acknowledgments

We would like to thank M Pepper and M J Kelly for very useful discussions. One of us, L Martin-Moreno, would like to thank the Comunidad de Madrid for financial support, and the Cavendish Laboratory for the use of their facilities and the hospitality I found there. The other, C G Smith, would like to thank the SERC for support.

References

Buttiker M, Imry Y, Landauer R and Pinhas S 1985 *Phys. Rev.* B **31** 6207
Economou E N and Soukoulis C M 1981 *Phys. Rev. Lett.* **46** 618
Fisher D S and Lee P A 1981 *Phys. Rev.* B **23** 6851
Kirczenow G 1988 *Solid State Commun.* **68** 715
—— 1989 *J. Phys.: Condens. Matter* **1** 305
Laux S E, Frank D J and Stern F 1988 *Surf. Sci.* **196** 101
Payne M C 1988 *J. Phys. C: Solid State Phys.* **21** L579
Smith C G, Pepper M, Ahmed H, Frost J E F, Hasko D G, Peacock D C, Ritchie D A and Jones G A C 1988 *J. Phys. C: Solid State Phys.* **21** L893–98
Stone A D and Szafer A 1988 *IBM J. Res. Dev.* **32** 384
Szafer A and Stone A D 1989 *Phys. Rev. Lett.* **62** 300
Thornton T J, Pepper M, Ahmed H, Andrews D and Davies G J 1986 *Phys. Rev. Lett.* **56** 1198
van Wees B J, can Houten H, Beenakker C W J, Williamson J G, Kowenhoven L P, van der Marel D and Foxon C T 1988 *Phys. Rev. Lett.* **60** 848
Wharam D A, Ekenberg U, Pepper M, Hasko D G, Ahmed H, Frost J E F, Ritchie D A, Peacock D C and Jones G A C 1989 *Phys. Rev.* **39** 6283
Wharam D A, Thornton T J, Newbury R, Pepper M, Ahmed H, Frost J E F, Hasko D G, Ritchie D A and Jones G A C 1988 *J. Phys. C: Solid State Phys.* **21** L209